Hindawi
Complexity
Volume 2023, Article ID 7953967, 19 pages
https://doi.org/10.1155/2023/7953967

Research Article

Fluid Flow Behavior Prediction in Naturally Fractured Reservoirs Using Machine Learning Models

Mustafa Mudhafar Shawkat,[1] **Abdul Rahim Bin Risal**,[1] **Noor J. Mahdi**,[2] **Ziauddin Safari**,[3] **Maryam H. Naser**,[4] **and Ahmed W. Al Zand**[5]

[1]*Department of Petroleum Engineering, School of Chemical and Energy Engineering, Faculty of Engineering, Universiti Teknologi Malaysia, Johor Bahru 81310, Malaysia*
[2]*Department of Civil Engineering, Al-Maarif University College, Ramadi, Iraq*
[3]*Department of Civil Engineering, Faculty of Engineering, Takhar University, Taleqan, Afghanistan*
[4]*Building and Construction Techniques Engineering Department, Al-Mustaqbal University College, Hillah 51001, Iraq*
[5]*Department of Civil Engineering, Faculty of Engineering and Built Environment, Universiti Kebangsaan Malaysia (UKM), Bangi 43600, Selangor, Malaysia*

Correspondence should be addressed to Ziauddin Safari; zia.safari2011@gmail.com

Received 3 June 2022; Revised 15 October 2022; Accepted 29 November 2022; Published 20 February 2023

Academic Editor: Mostafa Al-Emran

The naturally fractured reservoirs are one of the most challenging due to the tectonic movements that are caused to increase the permeability and conductivity of the fractures. The instability of the permeability and conductivity effects on the fluid flow path causes problems during the transfer of the fluids from the matrix to the fractures and fluid losses during production. In addition, these complications made it difficult for engineers to estimate fluid flow during production. The fracture properties' study is important to model the fluid flow paths such as the fracture porosity, permeability, and the shape factor, which are considered essential in the stability of fluid flow. To examine this, this research introduced new models including decision tree (DT), random forest (RF), K-nearest regression (KNR), ridge regression (RR), and LASSO regression model,. The research studied the fracture properties in naturally fractured reservoirs like the fracture porosity (FP) and the shape factor (SF). The datasets used in this study were collected from previous studies "i.e., Texas oil and gas fields" to build an intelligence-based predictive model for fluid flow characteristics. The prediction process was conducted based on interporosity flow coefficient, storativity ratio, wellbore radius, matrix permeability, and fracture permeability as input data. This study revealed a positive finding for the adopted machine learning (ML) models and was superior in using statistical accuracy metrics. Overall, the research emphasized the implementation of computer-aided models for naturally fractured reservoir analysis, giving more details on the extensive execution techniques, such as injection or the creation of artificial cracks, to minimize hydrocarbon losses or leakage.

1. Introduction

1.1. Background. Naturally fractured reservoirs are the result of natural processes that present the diastrophism and volume shrinkage that lead to fractures that have dispersed as a consistently linked network across the reservoir [1]. The tectonic processes have evolved in reservoirs, fractured reservoirs are frequently found in weak reservoir rocks with poor porosity [2]. Due to that, the fracture is extended and large, where it is often referred to as the large fracture [3]. If the granular porosity is high but the rocks are fragile, the fracture is relatively small and limited in quantity, often referred to as microfractures [1]. The naturally fractured reservoirs are different from the conventional reservoirs [4, 5]. In addition, the tectonic movements affected by the behavior of the fracture during transfer and production of the fluids flow due to the high conductivity and permeability of the natural fractures [6]. The conductivity and permeability of the fractures factor minimize the fracture porosity of the fluids that cause low storage capacity [6]. In contrast, the conductivity of the matrix increases storage capacity with low permeability, which causes an increase in the matrix porosity [7]. According to previous studies, matrix porosity is higher than fracture porosity in the naturally fractured reservoirs, which the fluids store in the matrix [8].

Multiphase flow modeling in naturally fractured reservoirs has been considered an issue for petroleum reservoir engineers [9, 10]. Warren and Root have shown a dual-porosity model which presents multiphase behavior in fractured reservoirs [11]. In the dual-porosity model, there are two characteristic regions: matrix and fracture [12]. The naturally fractured reservoirs present one of the most difficult reservoirs in the petroleum industry due to the fracture properties like permeability and porosity, where the natural fracture permeability is higher than the matrix permeability in a dual-porosity system [12]. The hydrocarbons flow from the matrix to the fractures and from these to the wellbore where the fractures cannot store these fluids, which cause fluid flow losses. An obstacle of the fluid flow can be seen in Figure 1 [13].

The motivation is always focused on developing a reliable mathematical model for modeling naturally fractured reservoir properties such as fracture porosity (FP) and the shape factor (SF). In the literature, ML models are one of the technologies that contribute to the systematization of fluid flow by forming speculative models based on hypotheses and equations modeling the properties of petroleum fluids [14]. Hence, the focus of the current investigation is to test different versions of ML models for the prediction of FP and SF. The models are built based on the characteristics of oil and gas, such as matrix porosity, permeability, pressure, and temperature.

1.2. Literature Review. Modeling of the naturally fractured reservoirs is one of the challenges due to the generation of the complex fractures and the conductivity factor of fractures that affect fluids paths [15]. Although fractures covered 20% of world reserves, naturally fractured reservoirs represented the risk reservoirs in drilling, production, and modeling processes due to fracture pressure that sometimes-caused loss in hydrocarbons production [16]. Two studies were conducted to investigate the naturally fractured reservoirs functionally [11, 17]. Both studies relied on the modeling of the naturally fractured, double-connected system, which was divided into two areas, the matrix and the fracture. The authors concluded that the fracture is central to the permeability of hydrocarbons and that the fluid flows from the matrix to the fracture depending on the geometric parameters of the fracture such as permeability and porosity [18]. Li et al. [19] extended the study of fluid leakage in areas of tectonic stress. To examine this, the tectonic movements affected the fracture behavior, which causes losses in the fluids of low-permeability formations. This examined some of the factors affecting the leakage of fluids by making a model for analyzing the leakage of fluids in naturally fractured gas fields. Turn to Warren and Root [11], the authors have provided a suitable solution to this problem and were able to arrive at these parameters, the actual shape, dimensions, and fluid flow properties of the reservoir, where the same scenario had been adopted later in [20, 21].

Two quadruple porosity models (QPM) that include a triple-fracture network with a single matrix system were presented by Dreier et al. [22] for naturally fractured reservoirs (NFR). The pressure-transient features of QPM are analysed and evaluated using these models: Warren and Root theory with various forms of matrix-to-fracture flow regimes, wellbore storage, and skin are commonly employed in well-test analysis, and the parameters storativity ratio and interporosity flow coefficient are significant in describing such reservoirs. Perez Garcia [23] improved the earlier simulation-based investigations, relying mainly on the Warren and Root equations as well as the Gilman model. The author came to the conclusion that the well-test data was reliable but more investigations and development assumptions were required for fracture reservoirs.

In order to boost the productivity of naturally fractured reservoirs, acid fracturing procedures are used. The effectiveness of the therapy is influenced by a number of factors, including treatment circumstances and reservoir characteristics. It is possible to measure the effectiveness of acid fracturing stimulations using a variety of methods [24]. Only a few models, however, took into account the natural fractures (NFs) present in the hydrocarbon reservoirs [25], using an ML model. Hence, the goal of this work is to develop an effective model to calculate the efficacy of acid fracturing therapy in naturally fractured reservoirs. This study estimates the increase in hydrocarbon production brought on by the use of acid fracturing treatments and takes into account the interactions between naturally occurring and artificially generated cracks. The reservoir features and treatment parameters of more than 3000 scenarios were utilized to create and validate the artificial neural network (ANN) model [26]. The created model takes into account the formation permeability, injection rate, natural fracture spacing, and treatment volume as reservoir and treatment characteristics [27]. To evaluate the effectiveness of the model's prediction, the percentage error and correlation coefficient were also calculated. The performance of acid fracturing treatments can be predicted quite accurately using the proposed model. The testing datasets yielded a correlation coefficient of 0.94 and a percentage error of 6.3%.

A novel ML model based on an improved learning process was established to offer a precise and timely forecast for increased productivity [28]. In order to assess the validity of the new equation, validation data were employed. A 6.8% average absolute error and a 0.93 correlation coefficient were obtained, demonstrating the excellent dependability of the suggested correlation. The originality of this work is in creating a solid and trustworthy model to forecast productivity gains from acid fracturing in naturally fractured reservoirs. By offering quick and accurate calculations, the novel correlation can be used to enhance the treatment design for naturally fractured reservoirs [29]. In order to

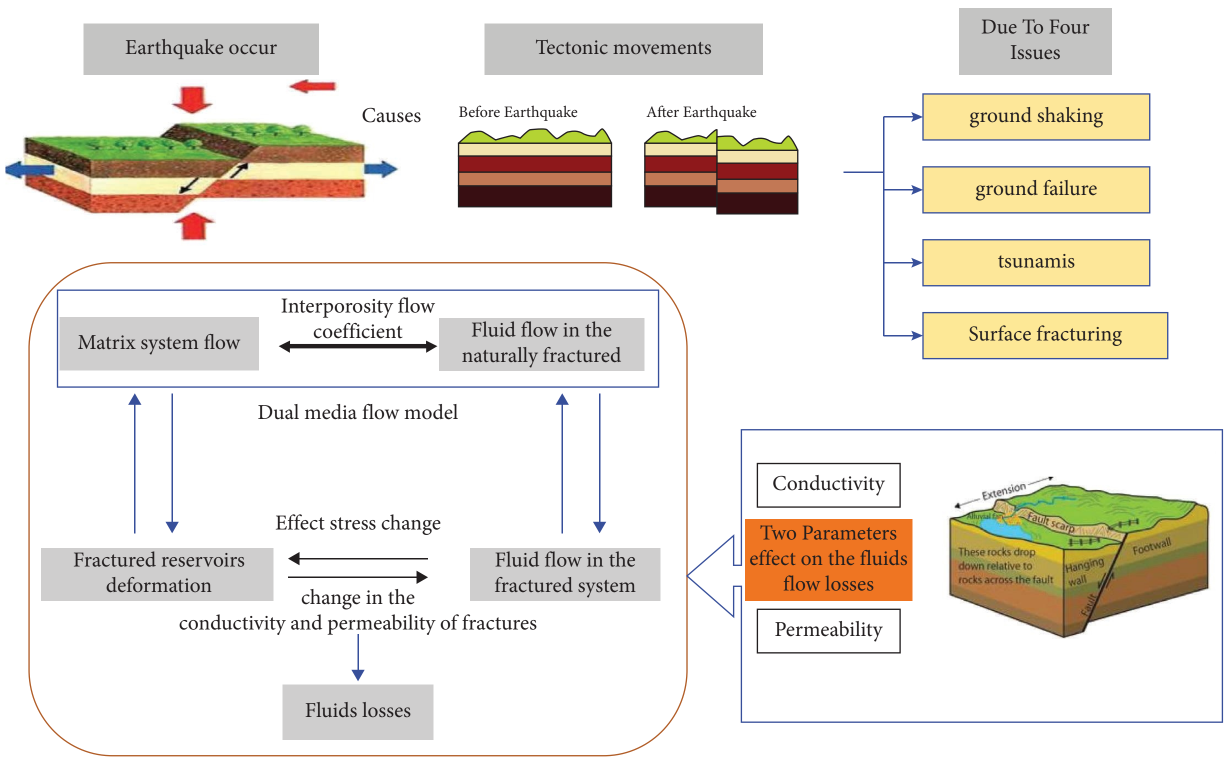

FIGURE 1: Fluid flow losses in the naturally fractured reservoirs.

estimate fracture permeability under complex physics, an integrated workflow based on the ML model was proposed (e.g., inertial effect) [30]. The methodology is being used for the first time to scale up rocks [31]. The suggested model provides a practical and accurate replacement for conventional upscaling techniques that can be quickly integrated into workflows for reservoir characterization and modeling.

Analysis of pressure-transient well tests is a crucial technique for figuring out reservoir properties [32]. Due to the analysts' inexperience, the validity of the data from the well-test analysis could be questioned [33]. A one-dimensional convolutional neural network (1D CNN) was tested to create an autonomous model for well-tested data interpretation [34]. Both the associated parameters and the type of curve can be automatically identified by the model [35]. Without adjusting the model architecture or using hyperparameters, a combined automatic interpretation model with four conventional well-test models were conducted. According to the findings, the 1D CNN model outperformed the ANN model. Three field cases are used to further validate the automatic interpretation model. Based on the reported literature review, the current research was inspired to develop a new methodology based on a soft computing model that is associated with theoretical study in the conditions of simulation data as well as being specialized based on the assumptions [36]. Our paper focuses to solve the fluids losses problem by modeling the fluids flow in the fractured reservoirs through using machine learning technique. This paper depends on the two parameters which are interporosity flow coefficient and storativity ratio to determine the fluid flow behavior.

1.3. The Objective of This Study. The previous studies used empirical methodologies and modern models such as ML models for diverse oil and gas datasets. This leads to the continuous issue in fluid flow paths due to the changes of the fracture's characteristic such as high conductivity and permeability of fractures. In conjunction with modern technology, the aim of this research is to make use of the applicability of ML models for predicting the shape factor and the fracture porosity. The models evaluated the fluid flow in the naturally fractured reservoirs. Predictive models were established using five different related input parameters. The assumption of the characteristics of the oil and gas datasets allows the ML models to build more than one model for the same datasets and compare them to get the best two models. The expected research outcome is to develop a reliable alternative technology for the petroleum industry where it can participate in sustainability and management.

2. Data Descriptions

This study specializes in analyzing the fluid flow behavior in naturally fractured reservoirs during production. The actual data consist of oil and gas data were obtained from Texas field. The actual data take account of the matrix permeability, fracture permeability, wellbore radius, interporosity flow coefficient, and the storativity ratio as inputs while the fracture porosity as outputs. To accomplish that, the study changed the input and output of Texas field data such that storativity ratio, interporosity flow coefficient, matrix permeability, fracture permeability, and wellbore radius are input data, while the shape factor and fracture porosity are output data. The conditions of input and output data were put as temperature 150 Fahrenheit, pressure 3,626 psi, and matrix porosity 22% for oil and 15% for gas, radius 1,000 ft, where these conditions are the same as Texas field's conditions with some changes in the assumptions [23]. These data are implemented on the basis that the flow is radial, taking into account that there is no Darcy's law and no skin factor [37].

3. Machine Learning Methods

This section presented the utilized ML models adopted for fluid flow data simulation. ML models are built to describe the effect of the shape factor and the fracture on the treatment of the hydrocarbon's leakage. Five different types of ML models were developed, including decision tree regression, random forest regression, LASSO regression, K-N neighbors' regression, and ridge regression models. Figure 2 presented the flowchart of the conducted methodological mechanism for this study.

3.1. Decision Trees Model. Decision tree regression (DT) was developed by [38] as a powerful ML model for both classification and regression tasks [39, 40]. In the DT algorithm, features (extracted from a specific dataset) are arranged in a symbolic tree-shaped manner, with terminal and internal nodes representing leaves and splits, respectively [41]. A tree is shaped by following a set of fundamental principles. Multiple trees are combined to form a set of rules that can be used in the prediction step. The technique first builds a tree from the training dataset, after which it splits the original data into two branches using a binary split procedure. The new growth branches are subjected to the separation process, and this is continued when a new branch becomes inseparable, and the accompanying node achieves the minimum size and evolves into a terminal node [42]. DTR's principles are easy to understand and follow a logical pattern that can be described as a tree; this is a significant advantage of the DT over other models. However, despite being quicker than other AI models, DTR frequently is not the right choice for time-series problems [43] because it frequently does not generate accurate results when there are issues of nonlinearity or noisy datasets.

3.2. Random Forest Model. Random forest model was first developed by [44], and since its introduction, it has been used widely in many fields of science and engineering for prediction purposes [45–47]. The RF model is strongly advised for scenarios with numerous input variables. Regarding a random vector, RF is an individual uniform distribution to each tree in the forest. Although RF is preferred when the trees, *eta*, and *mtry* are of an appropriate size, the maximal depth can be adjusted according to the complexity of the data [48]. The RF model in this study was built using *library (random forest)*. The significant hyperparameters, such as *ntree*, *eta*, *max depth*, and *mtry*, were set to 140, 4, 6, and 2 accordingly in order to reduce overfitting issues. When regression trees are built using distinct bootstraps for each tree, the potential features in those trees can be modeled using such algorithms [49]. For the purposes of predicting the targeted parameters, every tree in the forest was treated equally. The first set was utilized for the growth of the trees and then for the assessment of each tree's classification error [50]. The RF prediction's output is represented thus,

$$y = \frac{1}{n_{\text{tree}}} \sum_{i=1}^{n_{\text{tree}}} y_i(x), \tag{1}$$

where y = the average prediction output from the overall number of trees and $y_i(x)$ = the trees' discrete prediction for output vector x. Model overfitting was avoided by using the ten-fold cross-validation procedure thrice. The tree was initially built for each predictor and was then followed-up with its growth to ensure optimal weight and minimal computed error. The significance of the predictors, as well as the self-adjusted growth of the selected trees, must be ranked using the RF approach. The RF model performed well across all the response predictors based on the employed performance indicators.

3.3. K-Nearest Neighbor Regression Model. The KNR classification was developed as a relatively new technique for the parametric estimation of unknown probabilities [51]. The KNR was mainly built for classification patterns with an understanding of the K-nearest neighbor rule [52]. The KNR concept relies on the distance between the distributions to categorize each piece of data that contains the majority of nearest neighbors [53]. The prediction process of KNR depends on the use of classifiers and regression, wherein the regression aspect uses previously processed data to predict future data. Statistical methods, such as linear regression, are typically used to process the regression; however, the use of the linear regression method is limited only to some databases. This study implemented regression for the prediction of the fracture porosity and the shape factor based on gas and oil filled data observations. The problem with regression is predicting the result of a preprocessed parameter using a certain collection of independent variables. The result can be expressed as $G = G_n$ if the KNR is performed using n nearest neighbors. Then, the average of the results is used to determine the outcome. The solution will then be given as

$$G = \frac{G_n}{2}. \tag{2}$$

At that point, KNR prediction initiates the outcome of the neighbor, and prediction can be done by determining the Euclidean distance (ED) between the case point and the query based on the existing dataset.

$$D(z, q) = \sqrt{(z - q)^2}, \tag{3}$$

where z represents the query point and q represents the case point from the existing dataset.

3.4. Ridge Regression Model. In conditions whilst linearly impartial variables are closely correlated, RR model is a way of calculating the coefficients of a couple of regression fashions [54]. It has been applied in different engineering

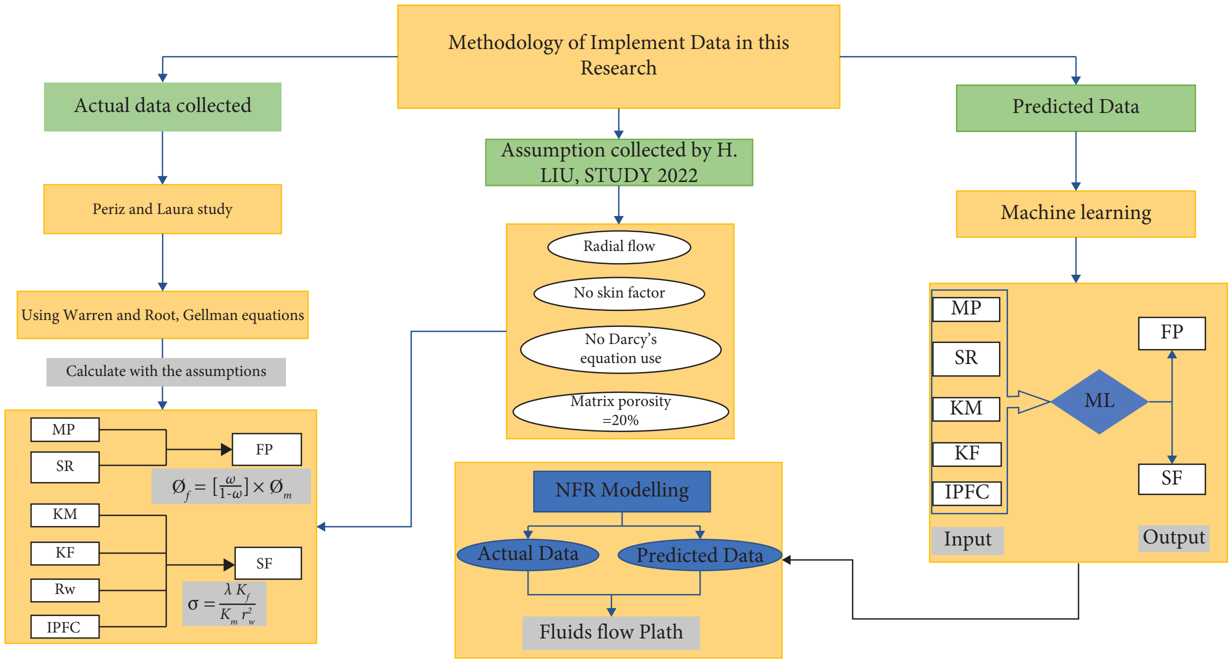

Figure 2: Methodology of databases modeling application.

and science domains and approved for its capacity. Amongst different areas and patterns of the RR model, equations are presented as follows [55]:

$$\widehat{B} = (X^T X)^{-1} X^T y, \quad (4)$$

where X^T is the transpose of X. By contrast, the ridge regression estimator to evaluate $(\widehat{B})$ the fracture porosity.

$$M_{\text{ridge}} = \left(X^T \widehat{X} + KIp\right)^{-1} X^T y, \quad (5)$$

where Ip is the $p \times p$ identity matrix, and $K > 0$ indicates a large number. The form along the diagonal of I is known as a ridge.

3.5. Lasso Model. Lasso is a commonly used sparse regression technique that relies on the sparse assumption for parameter regularization [56]. It is an innovative method for variable selection during regression tasks that operates by minimizing the residual sum of squares under the condition that the sum of absolute values of the coefficients is less than a constant [57]. It was first discussed in relation to least squares. The following is a summary of the basic Lasso framework. Assume a sample of N cases with p variables and a single outcome for each of the N instances. Consider that y_i is the response variable while $x_i = (x_1, x_2, x_3, \ldots, x_{np})$. T represents the covariate vector for the i^{th} case, $\beta = (\beta_1, \beta_2, \ldots, \beta_p)^T$. Hence, Lasso is aimed to solve the regression problem using nonlinearity functional properties.

4. Results and Discussion

In this section, the results of the adopted ML models were presented based on the radial flow in the fluid modeling of fracture reservoirs. Radial flow was concerned with the analysis of the flow of fluids along a radius. The volume for the wellbore radius is not large enough to cover the modeling of an entire well by ML models. The present results provide a slight improvement over the previous results of the data provided by Perez [23].

One of the most popular graphical presentation on the predictability evaluation is the scatter plot between the actual observations and the predictive models results, which was adopted here for assessment. All models were developed based on the predictability and interoperability of fluid flow losses. The modeling results for the DT model for the gas flow were reported in Figure 3 (Figure 3(a): fracture porosity, and Figure 3(b): shape factor). The DT model attained a determination coefficient ($R^2 \approx 0.80$) for fracture porosity and $R^2 \approx 0.94$ for the shape factor. This was formed in harmony with the established previous research of [23]. The modeling of Perez's data is assumed to be actual if our results build on the predicted data. On the other hand, the results for the oil flow characteristic are given in (Figure 4(a): fracture porosity ($R^2 \approx 0.93$) and Figure 4(b): shape factor ($R^2 = 0.94$)).

In the same manner, the scatter plots for the other ML models are (i.e., RF "Figure 5: gas flow and Figure 6: oil flow," KNR "Figure 7: gas flow and Figure 8: oil flow," RR "Figure 9: gas flow and Figure 10: oil flow" and Lasso "Figure 11: gas flow and Figure 12: oil flow"). The superior prediction accuracies were observed for the gas flow fracture porosity using the Lasso model over the testing phase with ($R^2 \approx 0.97$). However, gas flow shape factor prediction achieved using KNR ($R^2 \approx 0.96$). It is true that all models relative accomplished their results over ($R^2 = 0.85$) as an indicator for acceptable results. However, the motivation here is to target the more accurate model which is relatively near to the factual field observations with $R^2 \approx 1$. For the oil flow, the fracture porosity and shape factor were predicted accurately using the Lasso model.

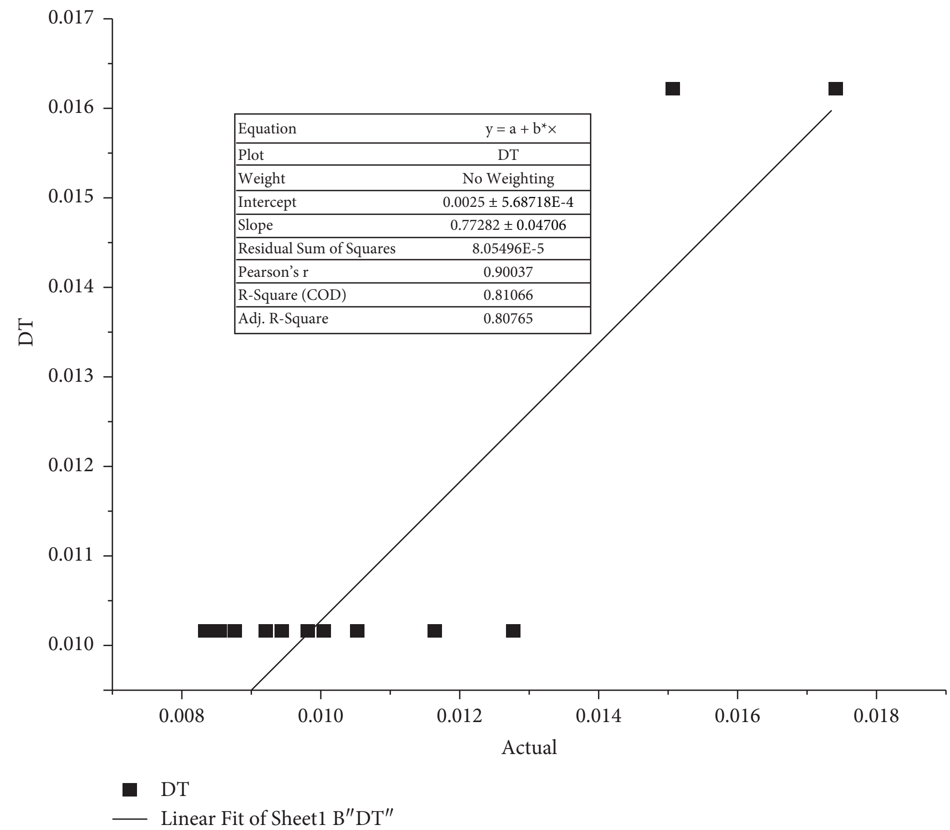

(a)

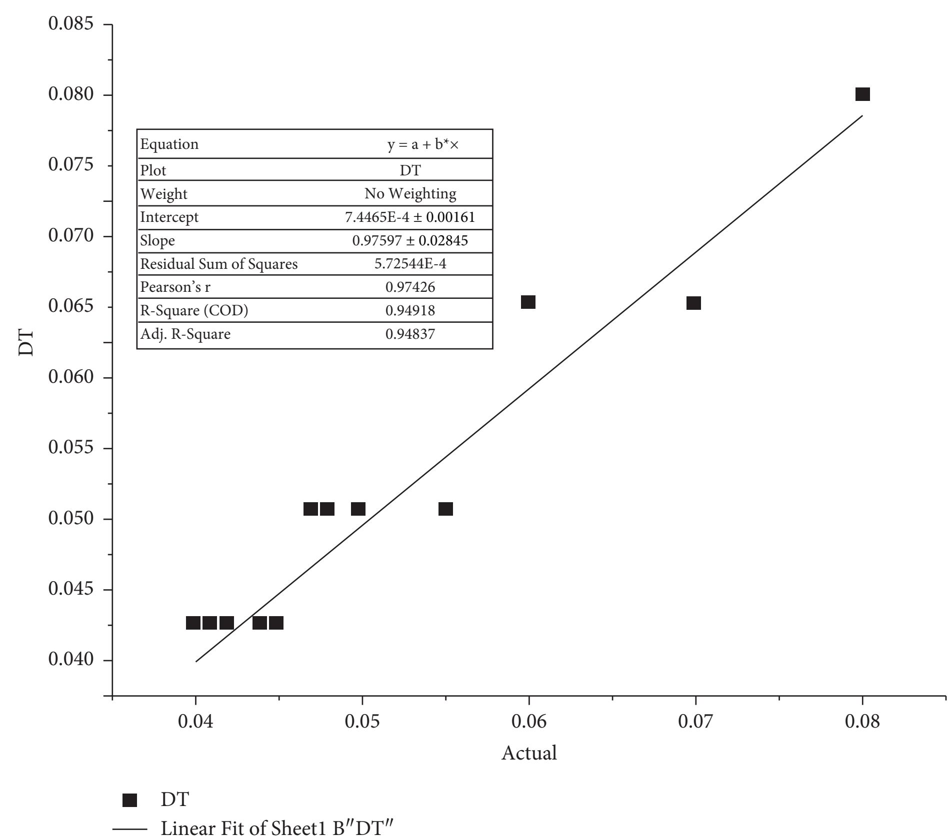

(b)

Figure 3: The decision tree model scatter plots for the testing phase of the gas flow: (a) fracture porosity and (b) shape factor.

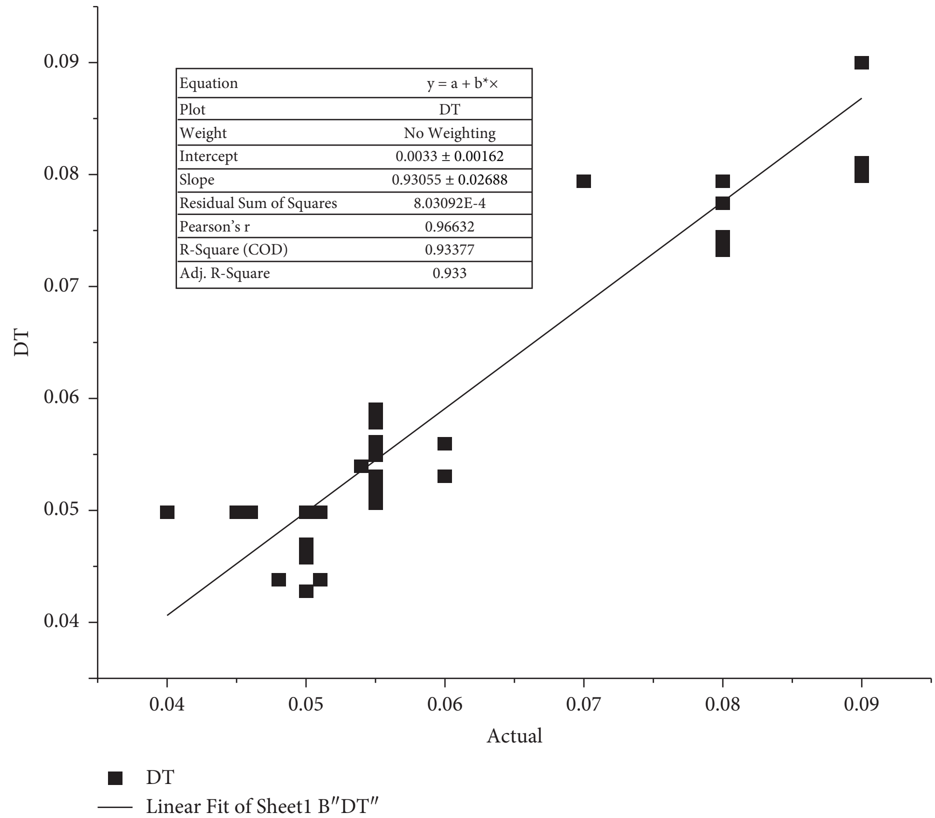

(a)

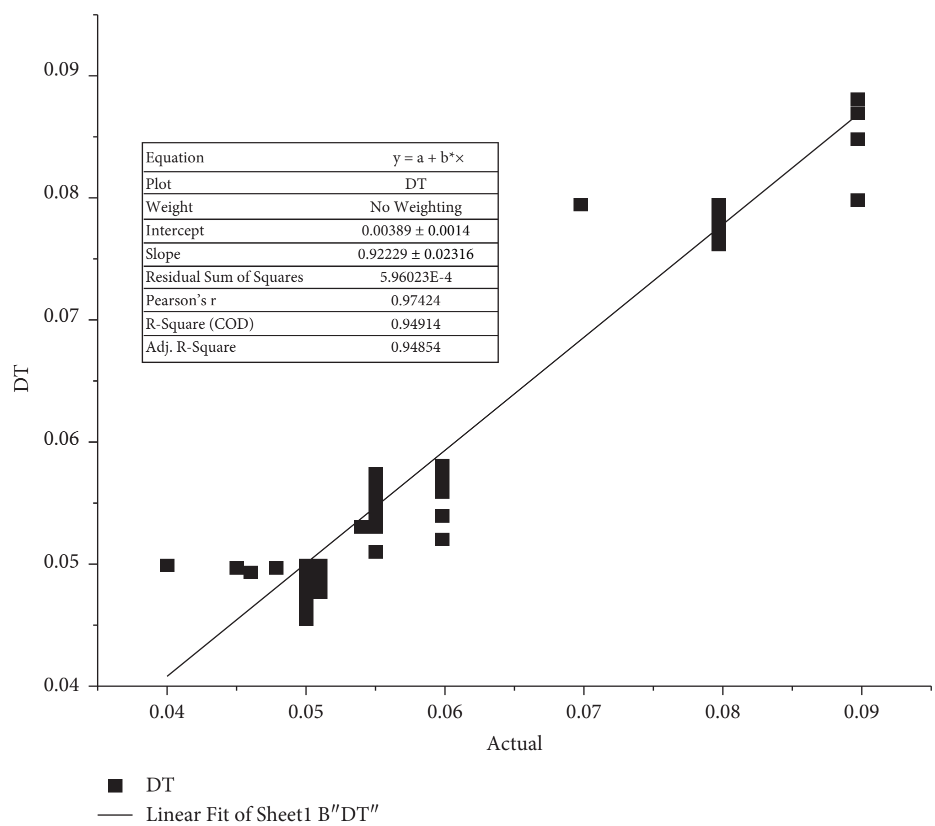

(b)

Figure 4: The decision tree model scatter plots for the testing phase of the oil flow: (a) fracture porosity in oil system and (b) shape factor.

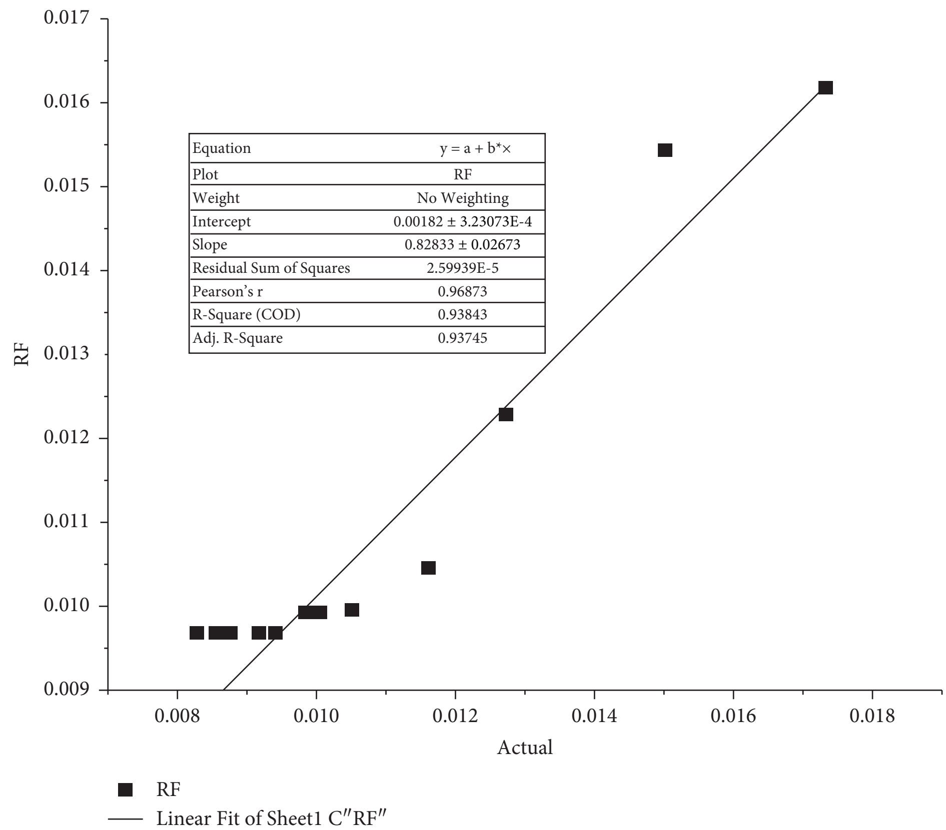

(a)

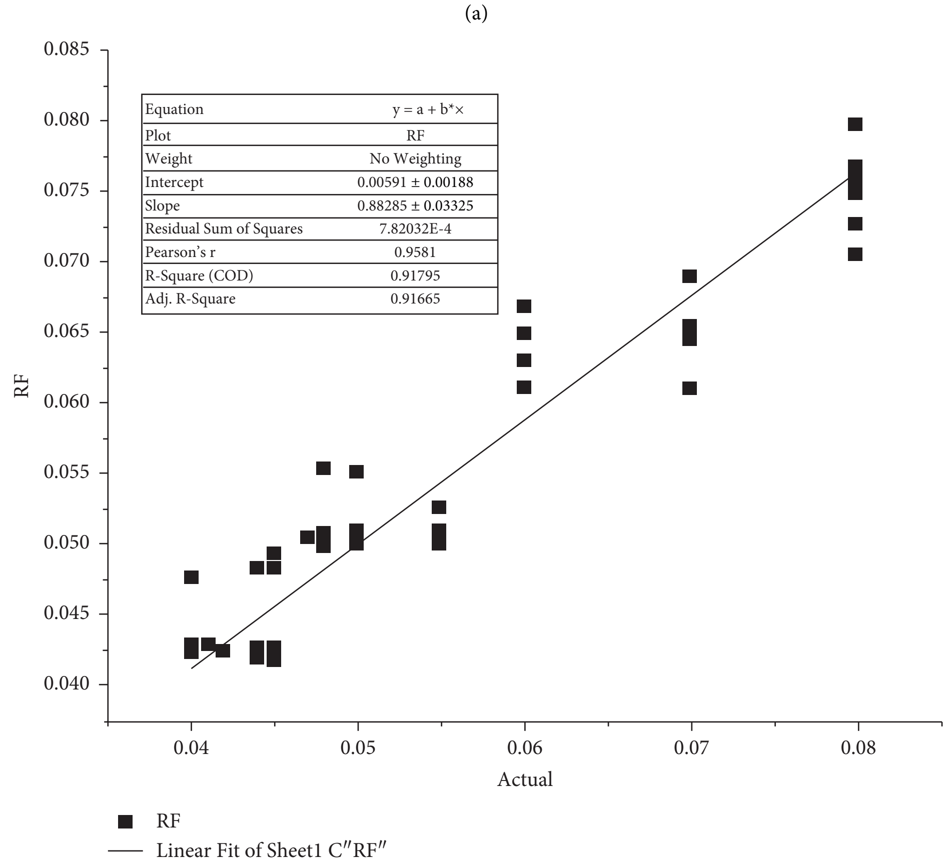

(b)

Figure 5: The random forest model scatter plots for the testing phase of the gas flow: (a) fracture porosity in oil system and (b) fracture porosity.

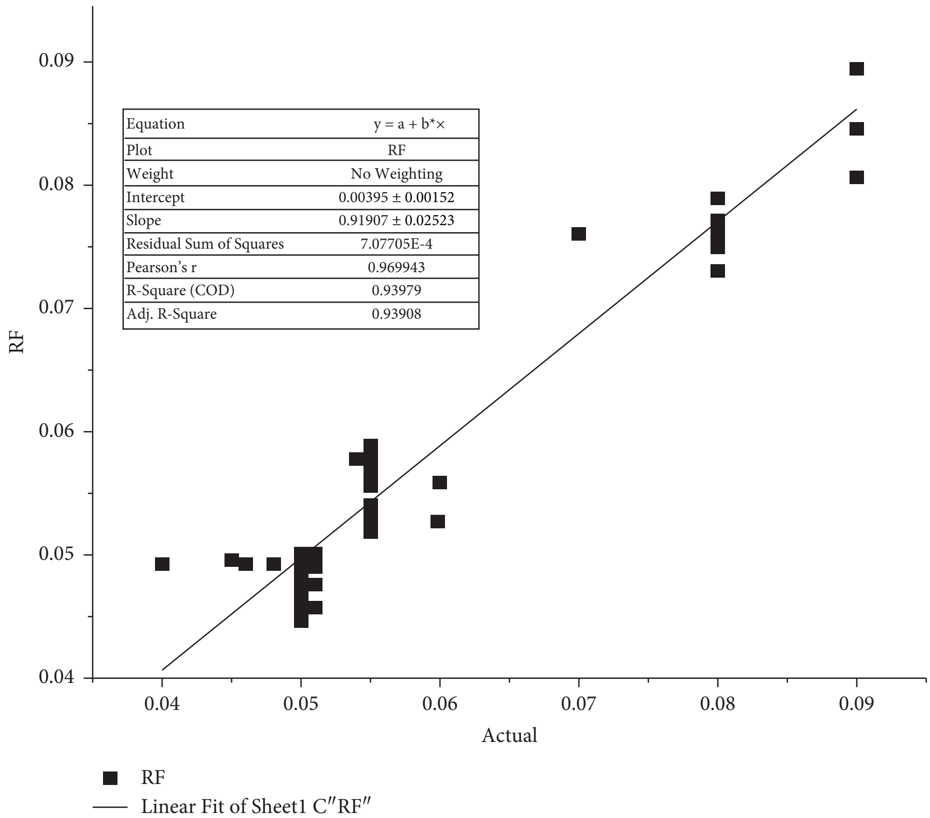

(a)

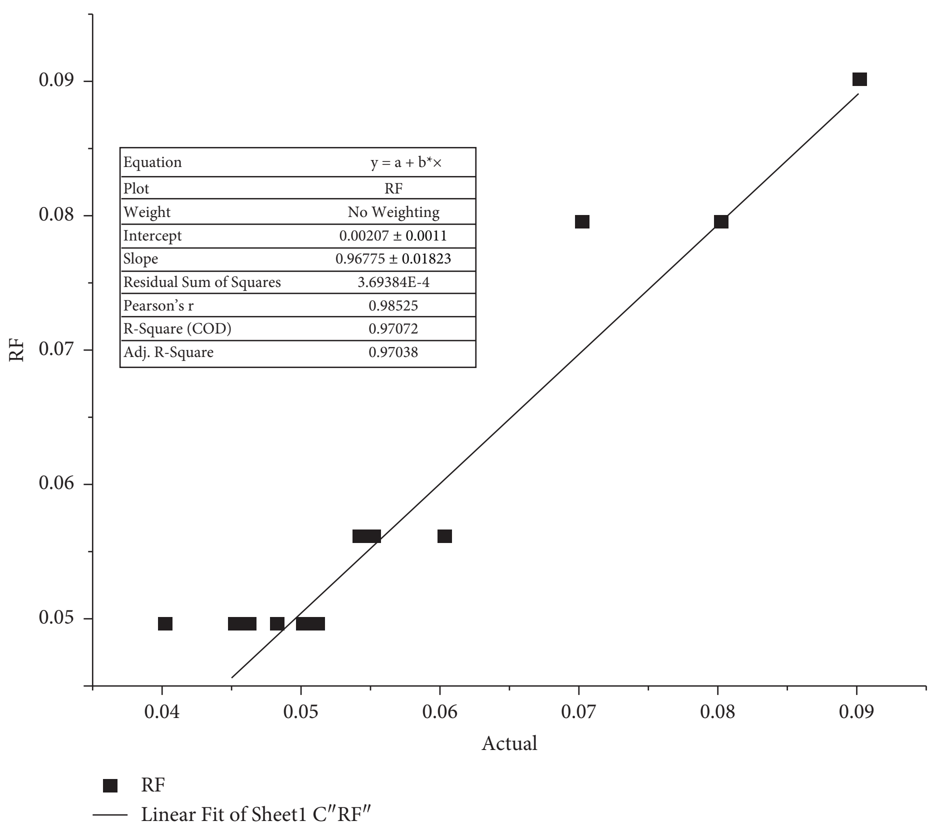

(b)

Figure 6: The random forest model scatter plots for the testing phase of the oil flow: (a) fracture porosity in oil system and (b) shape factor.

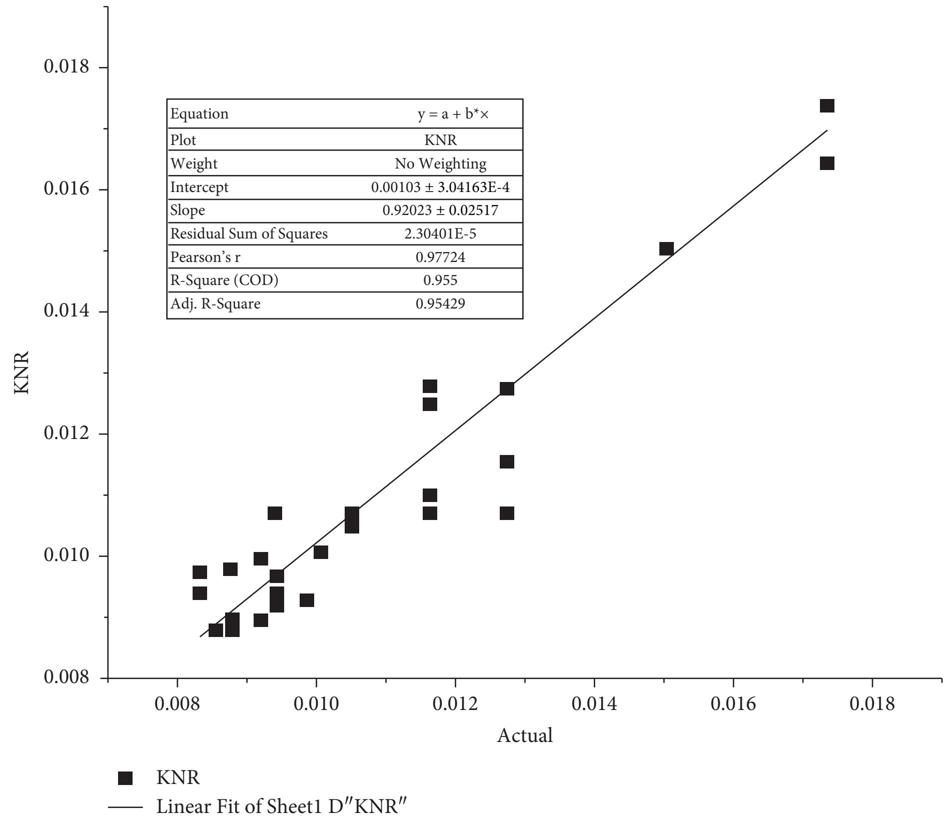

(a)

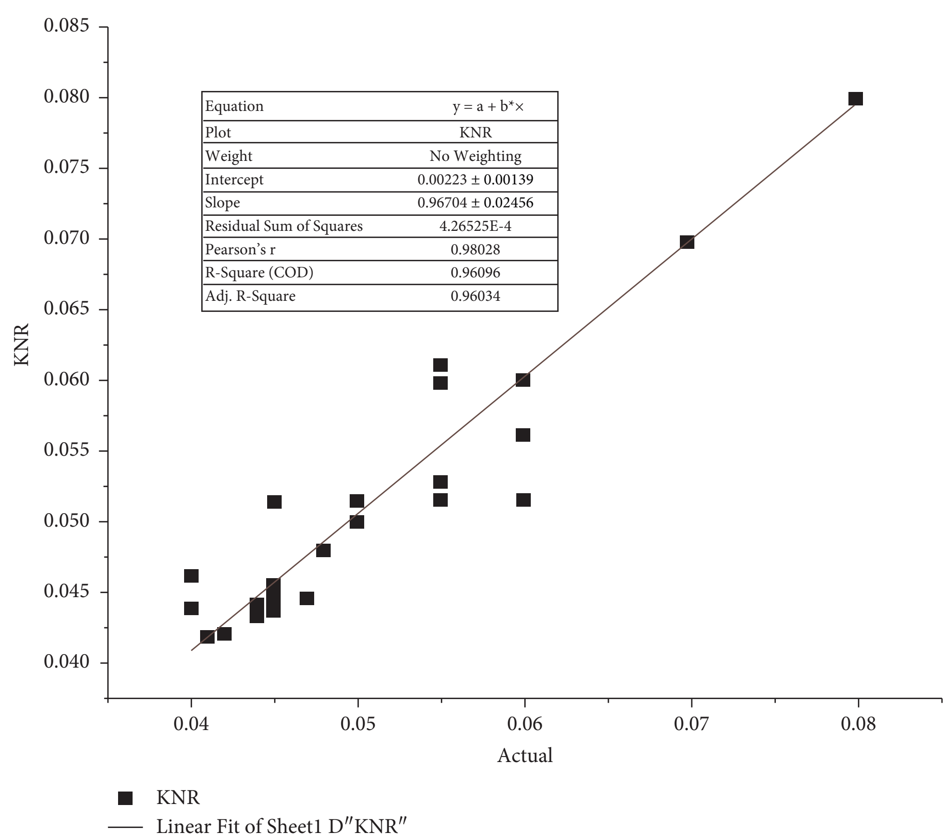

(b)

FIGURE 7: The K-nearest regression model scatter plots for the testing phase of the gas flow: (a) fracture porosity in oil system and (b) fracture porosity.

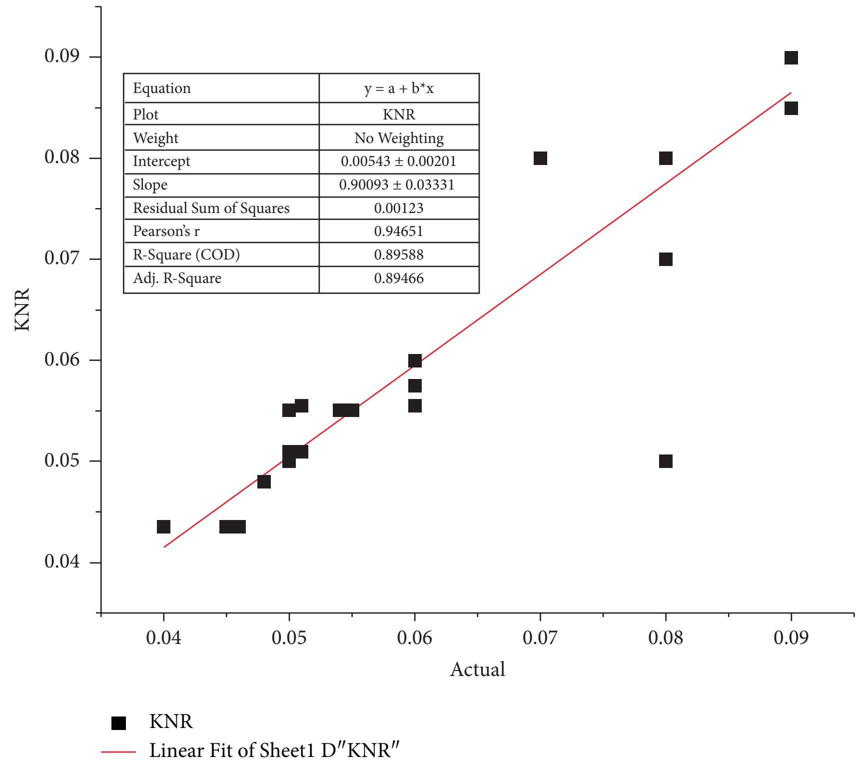

(a)

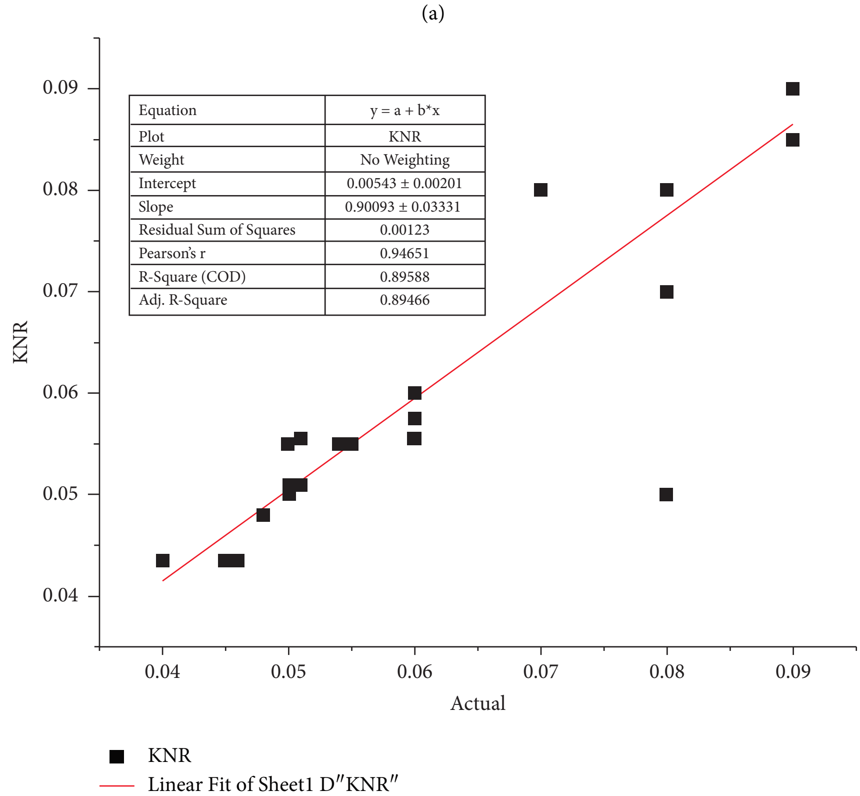

(b)

Figure 8: The K-Neighbor regression model scatter plots for the testing phase of the oil flow: (a) fracture porosity and (b) shape factor.

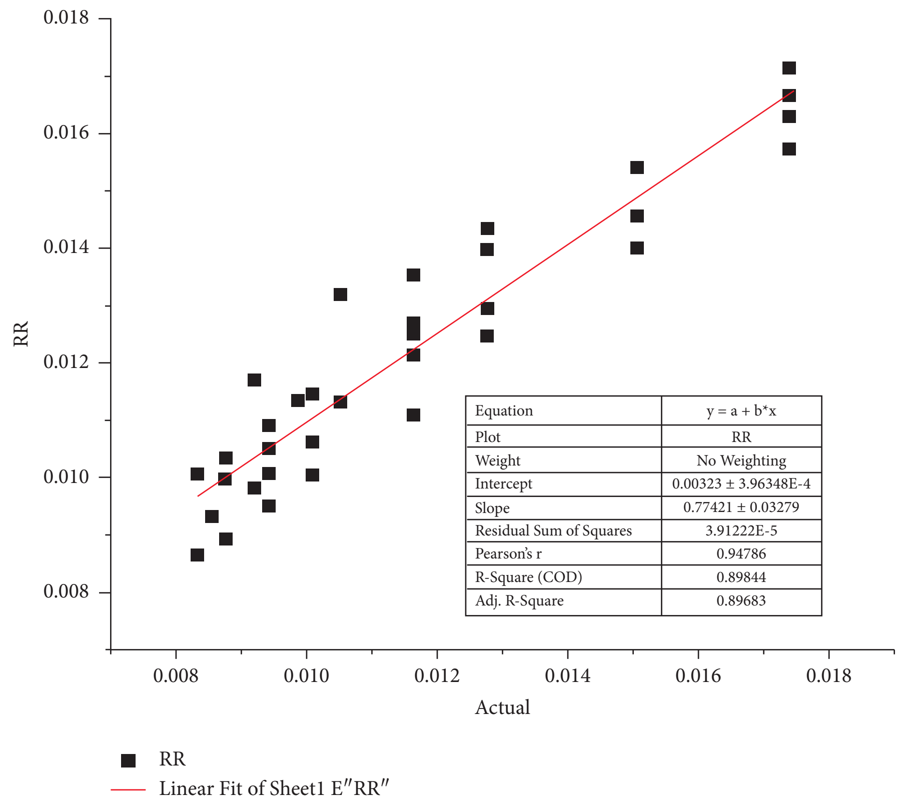

(a)

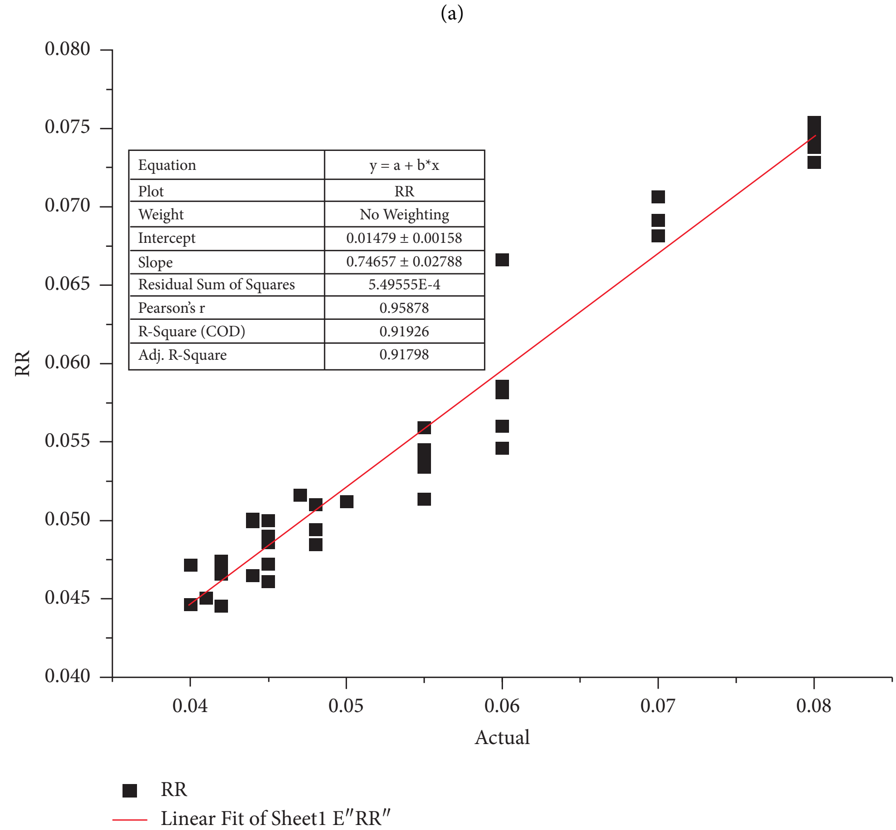

(b)

Figure 9: The Ridge regression model scatter plots for the testing phase of the gas flow: (a) fracture porosity in oil system and (b) fracture porosity.

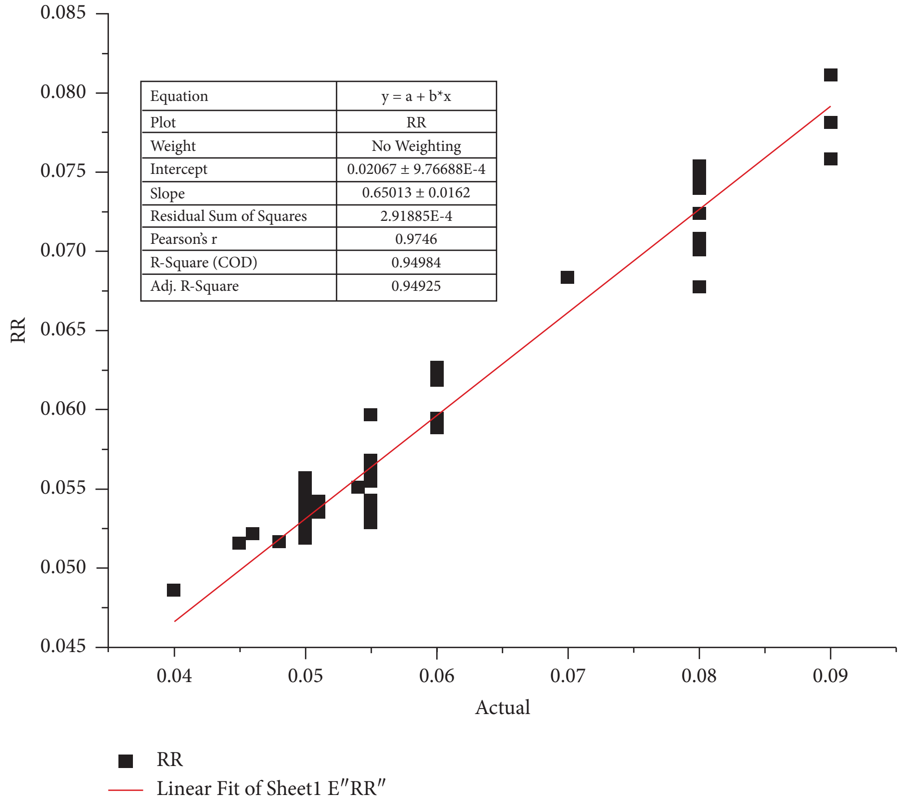

(a)

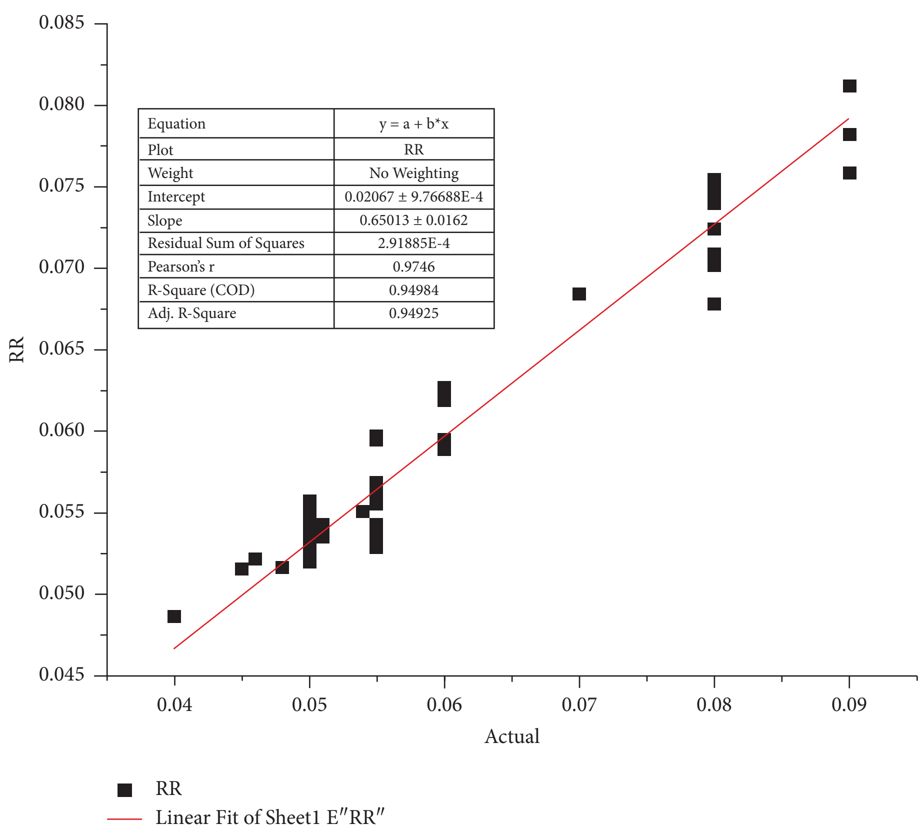

(b)

FIGURE 10: The Ridge regression model scatter plots for the testing phase of the oil flow: (a) fracture porosity and (b) shape factor.

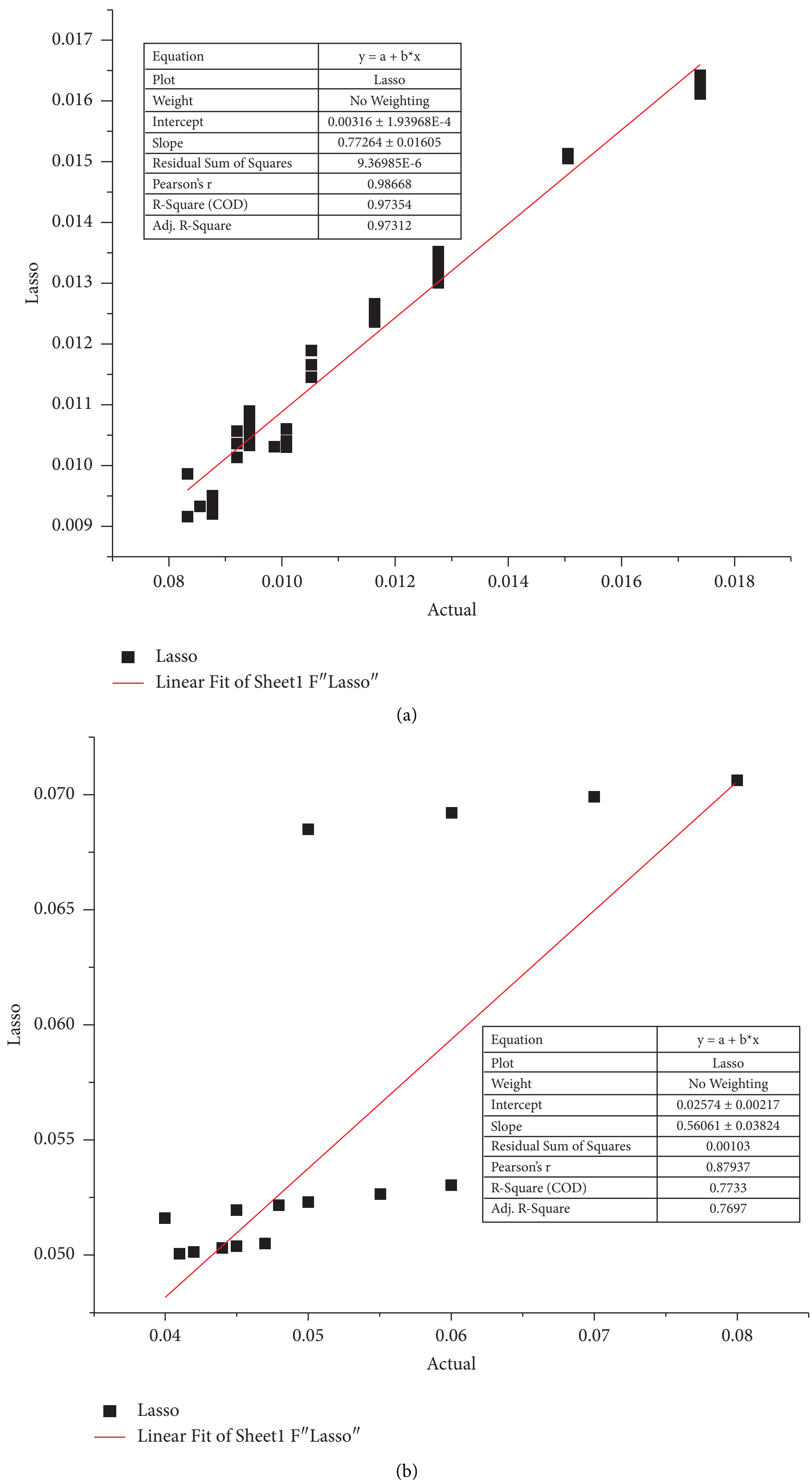

FIGURE 11: The Lasso model scatter plots for the testing phase of the gas flow: (a) fracture porosity in oil system and (b) fracture porosity.

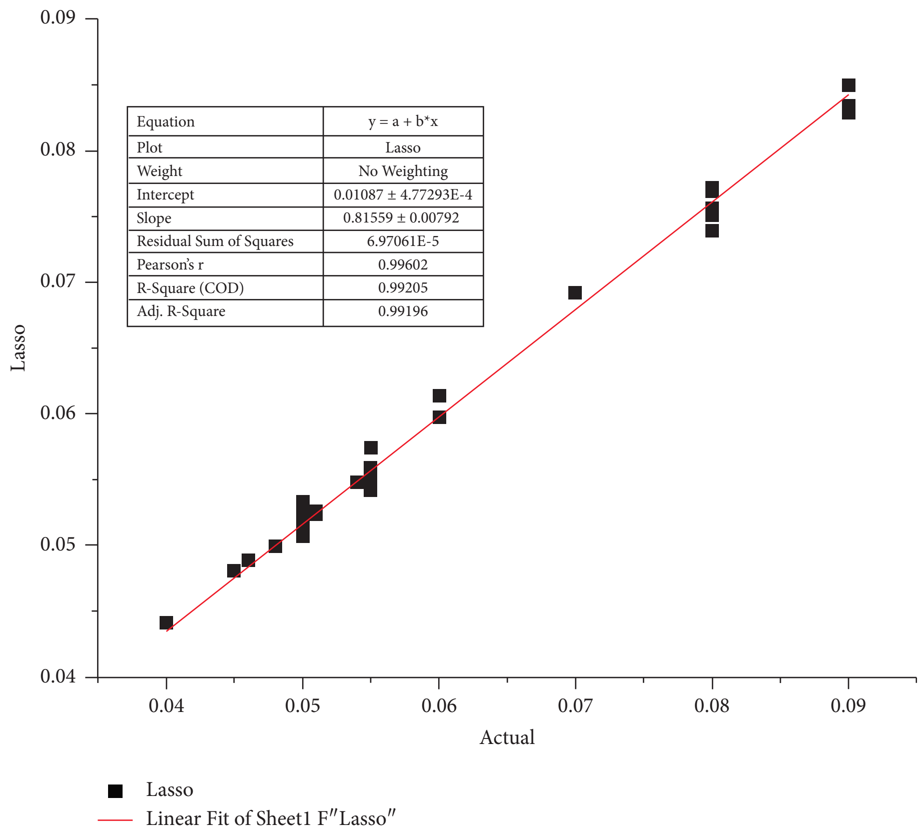

(a)

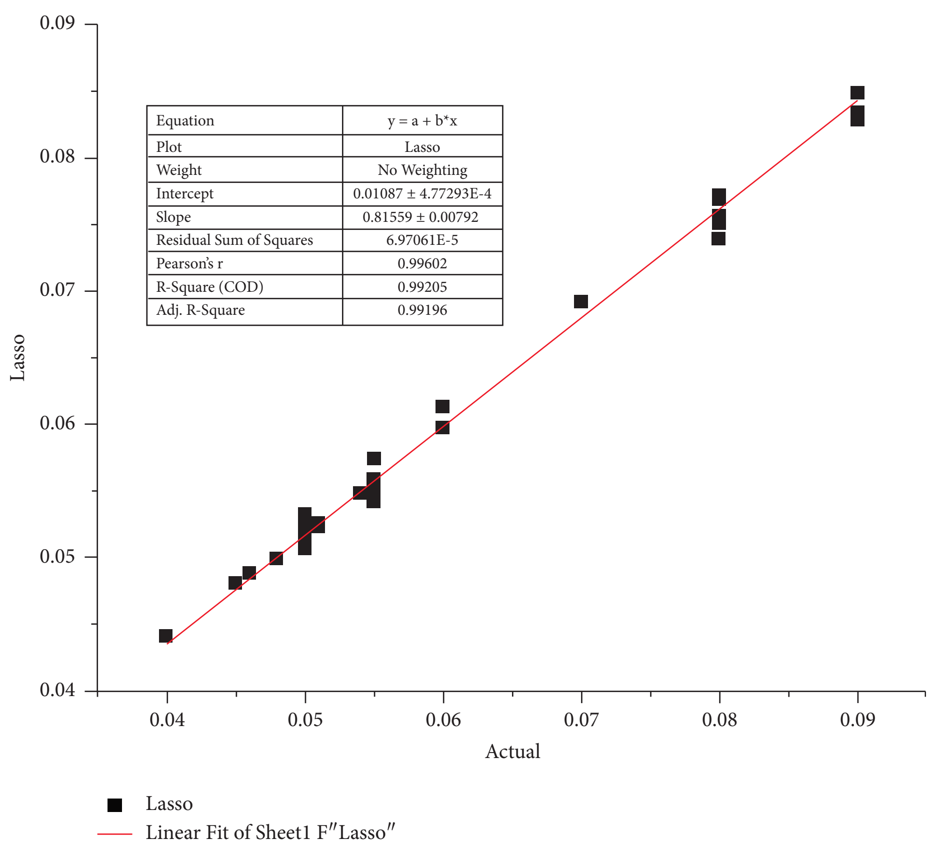

(b)

FIGURE 12: The Lasso model scatter plots for the testing phase of the oil flow: (a) fracture porosity and (b) shape factor.

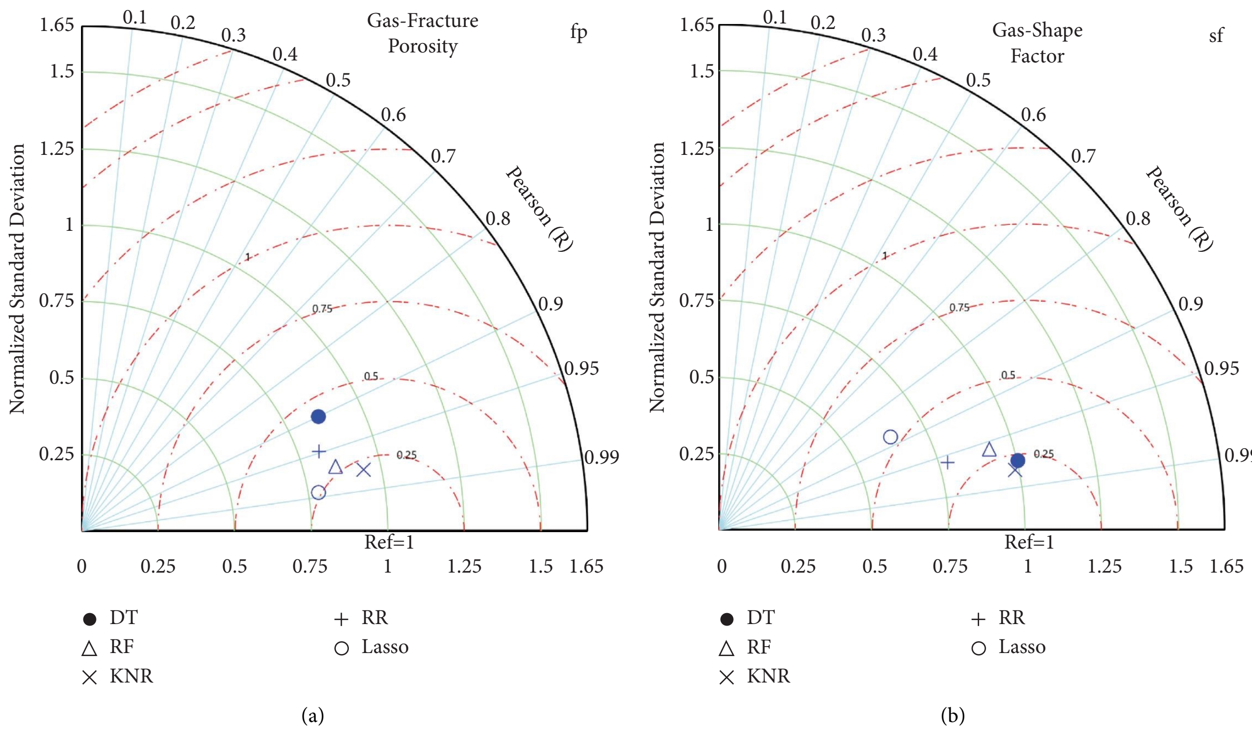

Figure 13: Taylor diagram presentation for the gas flow fracture porosity and shape factor prediction using different machine learning models.

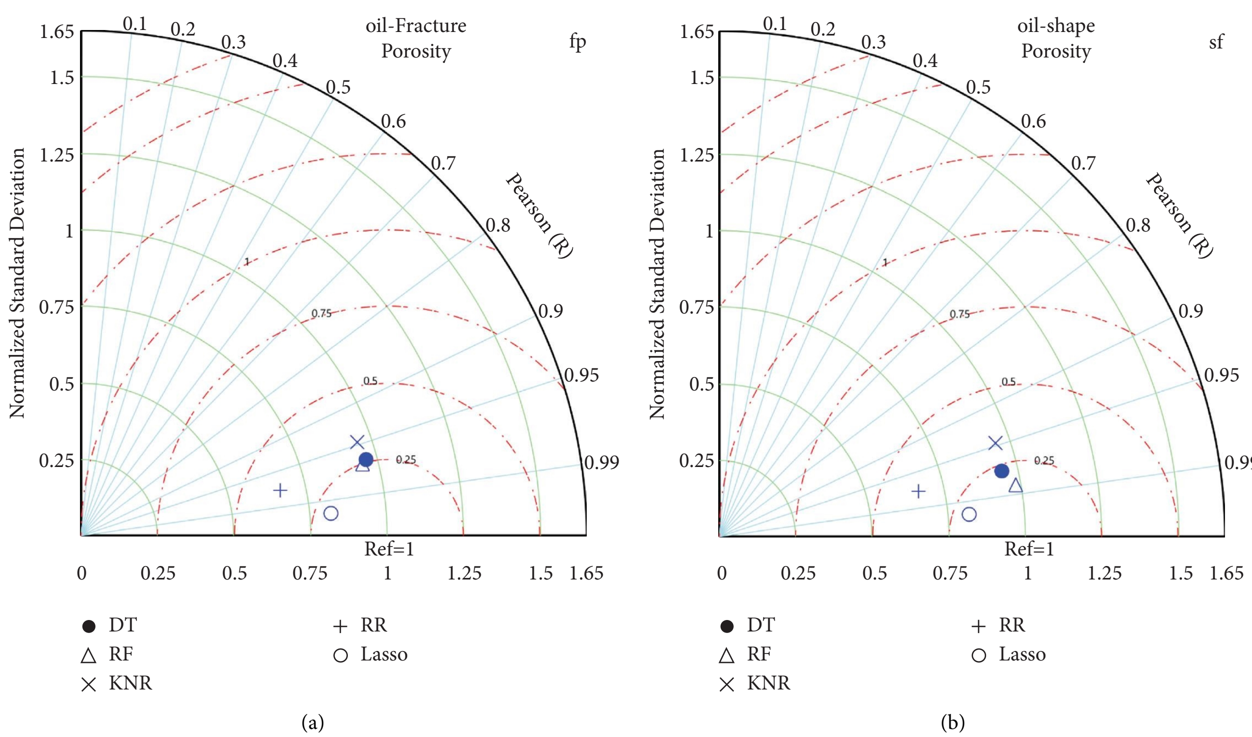

Figure 14: Taylor diagram presentation for the oil flow fracture porosity and shape factor prediction using different machine learning models.

Table 1: The calculated performance metrics for the gas flow fracture porosity over the testing phase.

Model	R^2	KGE	RMSE	MAPE (%)
DT	0.811	0.826	0.001	10.1
RF	0.938	0.851	0.001	6.4
KNR	0.955	0.937	0.001	4.1
RR	0.898	0.803	0.001	8.9
Lasso	0.974	0.779	0.001	7.7

Table 2: The calculated performance metrics for the gas shape factor over the testing phase.

Model	R^2	KGE	RMSE	MAPE (%)
DT	0.949	0.972	0.003	4.7
RF	0.918	0.91	0.004	5.8
KNR	0.961	0.975	0.003	2.8
RR	0.919	0.774	0.004	6.7
Lasso	0.773	0.617	0.007	11.7

Table 3: The calculated performance metrics for the oil fracture porosity over the testing phase.

Model	R^2	KGE	RMSE	MAPE (%)
DT	0.934	0.948	0.003	3.7
RF	0.94	0.938	0.003	4.1
KNR	0.896	0.927	0.004	1.9
RR	0.95	0.666	0.005	5.8
Lasso	0.992	0.819	0.002	3

Table 4: The calculated performance metrics for the oil shape factor over the testing phase.

Model	R^2	KGE	RMSE	MAPE (%)
DT	0.949	0.94	0.003	3.5
RF	0.971	0.977	0.002	2.3
KNR	0.896	0.928	0.004	1.9
RR	0.95	0.666	0.005	5.8
Lasso	0.992	0.819	0.002	3

It is even better to explore more logical and scientifically acknowledged graphical presentation of the developed ML models [58]. A graphical based on root mean square error (RMSE), correlation, and standard deviation was generated in Figures 13(a) and 13(b) "gas flow presented in the form of fracture porosity and shape factor" and Figures 14(a) and 14(b) "oil flow presented in the form of fracture porosity and shape factor." Based on Figure 13(a), the KNR model presented the closest coordinate to the actual observation of gas flow fracture porosity. However, the prediction of gas flow shape factor was visualized using DT and KNR "relatively close coordinates" (Figure 13(b)). In Figure 14(a), Lasso models indicated nearer location for the fracture porosity; on the other hand, both models Lasso and RF showed relatively closer prediction performance for the shape factor of the oil flow (Figure 14(b)).

The modeling results further assessed using some statistical metrics based on the perfect fit of goodness (i.e., determination coefficient (R^2) and Kling–Gupta efficiency (KGE)) and absolute error indicators (i.e., root mean square error (RMSE) and mean absolute percentage error (MAPE)) [59]. Tables 1 and 2 reported the modeling results for the gas flow fracture porosity and shape factor, respectively. By examining all the performance metrics of the Table 1, it clearly appears that performing more than two or more statistical indicators can give more informative results of the adopted ML models. Although the Lasso model revealed the superior correlation value, the KNR model gave the minimal value for the MAPE metric in which by validating with KGE metric, it is clearly a valid model for prediction superiority for the fracture porosity of gas flow. On the other hand, Tables 3 and 4 presented the modeling results of the oil flow fracture porosity and shape factor, respectively. Over the testing phase, the KNR model reported the best modeling results for the fracture porosity and shape factor prediction based on the multiple metrics evaluation.

Based on the performance metrics in Tables 1–4, modeling superiority for the attained prediction results distributed between RF, KNR and Lasso models. Indeed, this is a factual thing for the ML models behavior through the learning process in which depending on the how much capacity can be attained during the learning mechanisms of the models. This can be elaborated also due to the distribution of the fracture points in one line which prove that the fracture conductivity factor has a big impact oil than gas [60]. Generally, the radial flow is distributed as parabolic that points of fluids spread systemically due to the shape factor in gas flow [61].

5. Conclusions

Reliably predicting distributed fluids flow in the naturally fractured reservoirs is achievable using ML models applied to a group of oil and gas datasets of Texas field calibrated with the fracture porosity and shape factor data. The fracture porosity and shape factor respond to the distinct characteristics of fractures such as conductivity and permeability factor in different ways. The results of this study lead to the following conclusions:

(i) When the fracture characteristics variables were used collectively in the trained models, it was definitively determining the suitable type of flow for oil and gas (pseudosteady state flow or radial flow).

(ii) Based on the five available input variables, the following two output variables are shown to be most effective when used in combination to predict the movement of the fluids in the naturally fractured reservoirs. These input variables are matrix permeability, fracture permeability, wellbore radius, interporosity flow coefficient, and storativity ratio, while the output variables are the fracture porosity and shape factor.

(iii) ML models confirmed their potential in predicting the ail/gas flow fracture porosity and shape factor.

(iv) Some limitations were observed that sometimes ML models cannot work well in the development of the behavior of the naturally fractured reservoir characteristics due to their instability in one pattern as same as conventional reservoirs and this causes it difficult to predict.

Data Availability

The data used to support the findings of this study are available from the corresponding author upon request.

Conflicts of Interest

The authors declare that they do not have any conflicts of interest.

References

[1] W. Narr, D. S. Schechter, and L. B. Thompson, "Naturally fractured reservoir characterization," *Society of Petroleum Engineers Richardson*, vol. 112, 2006.

[2] G. Penuela, E. A. Idrobo, A. Ordonez, C. E. Medina, and N. S. Meza, "A new material-balance equation for naturally fractured reservoirs using a dual-system approach," in *Proceedings of the SPE Western Regional Meeting 2001*, Richardson, TX, USA, March 2001.

[3] A. Ordonez, G. Peñuela, E.-A. Idrobo, and C. E. Medina, "Recent advances in naturally fractured reservoir modeling," *CT&F - Ciencia, Tecnología y Futuro*, vol. 2, no. 2, pp. 51–64, 2001.

[4] J.-C. Guo, R.-S. Nie, and Y.-L. Jia, "Dual permeability flow behavior for modeling horizontal well production in fractured-vuggy carbonate reservoirs," *Journal of Hydrology*, vol. 464, pp. 281–293, 2012.

[5] X. Du, Z. Lu, D. Li, Y. Xu, P. Li, and D. Lu, "A novel analytical well test model for fractured vuggy carbonate reservoirs considering the coupling between oil flow and wave propagation," *Journal of Petroleum Science and Engineering*, vol. 173, pp. 447–461, 2019.

[6] D. Li, W. Jiao, F. Yue, X. Xiang, and L. Pan, "Natural fractures and their effects on reservoir reconstruction in lower cambrian shale, southeast chongqing, China," *Energy Exploration and Exploitation*, vol. 33, no. 6, pp. 769–783, 2015.

[7] B. L. Beckner, *Improved Modeling of Imbibition Matrix/fracture Fluid Transfer in Double Porosity Simulators*, Stanford University, Stanford, CA, USA, 1990.

[8] M. Frey, C. Bossennec, L. Seib, K. Bär, E. Schill, and I. Sass, "Interdisciplinary fracture network characterization in the crystalline basement: a case study from the Southern Odenwald, SW Germany," *Solid Earth*, vol. 13, no. 6, pp. 935–955, 2022.

[9] H. K. Hawez, R. Sanaee, and N. H. Faisal, "A critical review on coupled geomechanics and fluid flow in naturally fractured reservoirs," *Journal of Natural Gas Science and Engineering*, vol. 95, Article ID 104150, 2021.

[10] H. Hawez, R. Sanaee, and N. H. Faisal, "Multiphase flow modelling in fractured reservoirs using A novel computational fluid dynamics approach," in *Proceedings of the 55th US Rock Mechanics/Geomechanics Symposium*, Houston, TX, USA, June 2021.

[11] J. E. Warren and P. J. Root, "The behavior of naturally fractured reservoirs," *Society of Petroleum Engineers Journal*, vol. 3, no. 3, pp. 245–255, 1963.

[12] J. R. Gilman, J. L. Bowzer, and B. W. Rothkopf, "Application of short-radius horizontal boreholes in the naturally fractured yates field," *SPE Reservoir Engineering*, vol. 10, no. 1, pp. 10–15, 1995.

[13] E. R. Rangel-German and A. R. Kovscek, "Matrix-fracture shape factors and multiphase-flow properties of fractured porous media," in *Proceedings of the SPE Latin American and Caribbean Petroleum Engineering Conference 2005*, Rio de Janeiro, Brazil, June 2005.

[14] P. C. Eze and L. Y. Hu, "Natural fracture presence prediction in unconventional reservoirs using machine learning and geostatistical methods - workflow and HFTS1 case," in *Proceedings of the 10th Unconventional Resources Technology Conference*, American Association of Petroleum Geologists, Denver, CO, USA, July 2022.

[15] A. Aghabarari and M. Ghaedi, "Evaluation of the effects of homogenizing matrix block sizes on the simulation of naturally fractured reservoirs," *Journal of Petroleum Science and Engineering*, vol. 213, Article ID 110373, 2022.

[16] B. E. M. Lima and L. F. De Ros, "Deposition, diagenetic and hydrothermal processes in the Aptian Pre-Salt lacustrine carbonate reservoirs of the northern Campos Basin, offshore Brazil," *Sedimentary Geology*, vol. 383, pp. 55–81, 2019.

[17] G. I. Barenblatt, I. Zheltov, and I. N. Kochina, "Basic concepts in the theory of seepage of homogeneous liquids in fissured rocks [strata]," *Journal of Applied Mathematics and Mechanics*, vol. 24, no. 5, pp. 1286–1303, 1960.

[18] H. Kazemi, L. S. Merrill, K. L. Porterfield, and P. R. Zeman, "Numerical simulation of water-oil flow in naturally fractured reservoirs," *Society of Petroleum Engineers Journal*, vol. 16, no. 6, pp. 317–326, 1976.

[19] Y. Li, J. Guo, J. Zhao, and Y. Yue, "A new model of fluid leak-off in naturally fractured gas fields and its effects on fracture geometry," *Journal of Canadian Petroleum Technology*, vol. 46, no. 12, 2007.

[20] H. Pulido, F. Samaniego, J. Rivera, R. Camacho, and C. Suárez, "Decline curve analysis for naturally fractured reservoirs with transient interporosity flow," in *Proceedings of the 27th Workshop on Geothermal Reservoir Engineering Stanford University*, Stanford, CA, USA, January 2002.

[21] S. Gerami, M. Pooladi-Darvish, and L. Mattar, "Decline curve analysis for naturally fractured gas reservoirs: a study on the applicability of pseudo-time and material balance pseudo-time," in *Proceedings of the International Petroleum Technology Conference*, Dubai, UAE, December 2007.

[22] J. Dreier, E. Ozkan, and H. Kazemi, "New analytical pressure-transient models to detect and characterize reservoirs with multiple fracture systems," in *Proceedings of the SPE International Petroleum Conference in Mexico*, Bakersfield, CA, USA, March 2004.

[23] L. E. Perez Garcia, *Integration of Well Test Analysis into Naturally Fractured Reservoir Simulation*, Texas A&M University, College Station, TX, USA, 2006.

[24] M. Akbari, M. Javad Ameri, S. Kharazmi, Y. Motamedi, and M. Pournik, "New correlations to predict fracture conductivity based on the rock strength," *Journal of Petroleum Science and Engineering*, vol. 152, pp. 416–426, 2017.

[25] M. S. Aljawad, M. P. Schwalbert, M. Mahmoud, and A. Sultan, "Impacts of natural fractures on acid fracture design: a modeling study," *Energy Reports*, vol. 6, pp. 1073–1082, 2020.

[26] M. S. Aljawad, M. P. Schwalbert, D. Zhu, and A. D. Hill, "Improving acid fracture design in dolomite formations utilizing a fully integrated acid fracture model," *Journal of Petroleum Science and Engineering*, vol. 184, Article ID 106481, 2020.

[27] M. S. Aljawad, H. Aljulaih, M. Mahmoud, and M. Desouky, "Integration of field, laboratory, and modeling aspects of acid fracturing: a comprehensive review," *Journal of Petroleum Science and Engineering*, vol. 181, Article ID 106158, 2019.

[28] Y. Chen, H. Wang, Y. Wang, and G. Ma, "Numerical evaluation of a fracture acidizing treatment in a three-dimensional fractured carbonate reservoir," *Journal of Natural Gas Science and Engineering*, vol. 81, Article ID 103440, 2020.

[29] A. M. Hassan, M. S. Aljawad, and M. A. Mahmoud, "Predicting the productivity enhancement after applying acid fracturing treatments in naturally fractured reservoirs utilizing artificial neural network," in *Proceedings of the Abu Dhabi International Petroleum Exhibition & Conference*, SPE, Abu Dhabi, UAE, November 2021.

[30] G. M. Lomize, "Water flow through jointed rock," *Gosenergoizdat, Moscow*, vol. 127, 1951 (in Russian).

[31] S. Marelli and B. Sudret, "UQLab: A framework for uncertainty quantification in matlab," *Vulnerability, Uncertainty, and Risk*, American Society of Civil Engineers, Reston, Virginia, USA, 2014.

[32] M. Alajmi and T. Ertekin, "The development of an artificial neural network as a pressure transient analysis tool for applications in double-porosity reservoirs," in *Proceedings of the Asia Pacific Oil and Gas Conference and Exhibition*, SPE, Jakarta, Indonesia, October 2007.

[33] O. F. Allain and R. N. Horne, "Use of artificial intelligence in well-test interpretation," *Journal of Petroleum Technology*, vol. 42, no. 3, pp. 342–349, 1990.

[34] A. M. AlMaraghi and A. H. El-Banbi, "Automatic reservoir model identification using artificial neural networks in pressure transient analysis," in *Proceedings of the SPE North Africa Technical Conference and Exhibition*, SPE, Cairo, Egypt, September 2015.

[35] A. A. Awotunde, "Estimation of well test parameters using global optimization techniques," *Journal of Petroleum Science and Engineering*, vol. 125, pp. 269–277, 2015.

[36] X. dong Wang, Y. fang Zhou, and W. jing Luo, "A study on transient fluid flow of horizontal wells in dual-permeability media," *Journal of Hydrodynamics*, vol. 22, no. 1, 2010.

[37] L. Mei, H. Zhang, L. Wang, Q. Zhang, and J. Cai, "Fractal analysis of shape factor for matrix-fracture transfer function in fractured reservoirs," *Oil & Gas Science and Technology*, vol. 75, p. 47, 2020.

[38] K.-M. Osei-Bryson, "Evaluation of decision trees: a multi-criteria approach," *Computers & Operations Research*, vol. 31, no. 11, pp. 1933–1945, 2004.

[39] A. Sharafati, S. B. Haji Seyed Asadollah, D. Motta, and Z. M. Yaseen, "Application of newly developed ensemble machine learning models for daily suspended sediment load prediction and related uncertainty analysis," *Hydrological Sciences Journal*, vol. 65, no. 12, 2020.

[40] A. Priyam, G. R. Abhijeeta, A. Rathee, and S. Srivastava, "Comparative analysis of decision tree classification algorithms," *International Journal of Current Engineering and Technology*, vol. 3, no. 2, pp. 334–337, 2013.

[41] S. Y. Kim and A. Upneja, "Majority voting ensemble with a decision trees for business failure prediction during economic downturns," *Journal of Innovation & Knowledge*, vol. 6, no. 2, pp. 112–123, 2021.

[42] M. Xu, P. Watanachaturaporn, P. K. Varshney, and M. K. Arora, "Decision tree regression for soft classification of remote sensing data," *Remote Sensing of Environment*, vol. 97, no. 3, pp. 322–336, 2005.

[43] G. K. F. Tso and K. K. W. Yau, "Predicting electricity energy consumption: a comparison of regression analysis, decision tree and neural networks," *Energy*, vol. 32, no. 9, pp. 1761–1768, 2007.

[44] L. Breiman, *Machine Learning*, vol. 45, no. 1, pp. 5–32, 2001.

[45] T. Tiyasha, T. M. Tung, S. K. Bhagat et al., "Functionalization of remote sensing and on-site data for simulating surface water dissolved oxygen: development of hybrid tree-based artificial intelligence models," *Marine Pollution Bulletin*, vol. 170, Article ID 112639, 2021.

[46] Z. M. Yaseen, Z. H. Ali, S. Q. Salih, and N. Al-Ansari, "Prediction of risk delay in construction projects using a hybrid artificial intelligence model," *Sustainability*, vol. 12, no. 4, p. 1514, 2020.

[47] M. Belgiu and L. Drăguţ, "Random forest in remote sensing: a review of applications and future directions," *ISPRS Journal of Photogrammetry and Remote Sensing*, vol. 114, pp. 24–31, 2016.

[48] S. Nickel, W. Schroder, W. Wosniok et al., "Modelling and mapping heavy metal and nitrogen concentrations in moss in 2010 throughout Europe by applying Random Forests models," *Atmospheric Environment*, vol. 156, pp. 146–159, 2017.

[49] A. O. Al-Sulttani, M. Al-Mukhtar, A. B. Roomi, A. Farooque, K. M. Khedher, and Z. M. Yaseen, "Proposition of new ensemble data-intelligence models for surface water quality prediction," *IEEE Access*, vol. 9, 2021.

[50] P. Zhang, R. P. Chen, and H. N. Wu, "Real-time analysis and regulation of epb shield steering using random forest," *Automation in Construction*, vol. 106, 2019.

[51] J. C. Bezdek, S. K. Chuah, and D. Leep, "Generalized k-nearest neighbor rules," *Fuzzy Sets and Systems*, vol. 18, no. 3, pp. 237–256, 1986.

[52] H. Samet, "K-nearest neighbor finding using MaxNearestDist," *IEEE Transactions on Pattern Analysis and Machine Intelligence*, vol. 30, no. 2, pp. 243–252, 2008.

[53] G. Batista and D. F. Silva, "How k-nearest neighbor parameters affect its performance," in *Argentine Symposium on Artificial Intelligence*, pp. 1–12, Citeseer, Princeton, NJ, USA, 2009.

[54] H. Tao, S. Q. Salih, M. K. Saggi et al., "A newly developed integrative bio-inspired artificial intelligence model for wind speed prediction," *IEEE Access*, vol. 8, pp. 83347–83358, 2020.

[55] M. H. J. Gruber, *Improving Efficiency by Shrinkage: The James-Stein and ridge Regression Estimators*, Routledge, Oxfordshire, UK, 2017.

[56] J. Ranstam and J. A. Cook, "LASSO regression," *British Journal of Surgery*, vol. 105, no. 10, p. 1348, 2018.

[57] R. Tibshirani, "Regression shrinkage and selection via the lasso," *Journal of the Royal Statistical Society: Series B*, vol. 58, no. 1, pp. 267–288, 1996.

[58] K. E. Taylor, "Summarizing multiple aspects of model performance in a single diagram," *Journal of Geophysical Research: Atmospheres*, vol. 106, no. 7, pp. 7183–7192, 2001.

[59] A. Botchkarev, "Performance metrics (error measures) in machine learning regression, forecasting and prognostics: properties and typology," 2018, https://arxiv.org/abs/1809.03006.

[60] S. Afzali, N. Rezaei, S. Zendehboudi, and I. Chatzis, "Computational fluid dynamic simulation of multi-phase flow in fractured porous media during water-alternating-gas injection process," *Journal of Hydrology*, vol. 610, Article ID 127852, 2022.

[61] A. Rossi, F. Alberini, and E. Brunazzi, "Identification of suspension state using passive acoustic emission and machine learning in a solid–liquid mixing system," *Chemical Engineering Research and Design*, vol. 177, pp. 273–282, 2022.